 doi:10.20944/preprints202209.0120.v1

Article

The Bioactive Phenolic Agents Diaryl Ether CVB2-61 and Diarylheptanoid CVB4-57 as Connexin Hemichannel Blocker

Anne Dierks [1], Corinne Vanucci-Bacqué [2,3], Anne-Marie Schäfer [1], Tina Lehrich [1], Frederike Ruhe [1], Patrik Schadzek [1], Florence Bedos-Belval [2,3] and Anaclet Ngezahayo [1,4,*]

[1] Leibniz University Hannover, Institute of Cell Biology and Biophysics, Dept. of Cell Physiology and Biophysics, Herrenhäuserstraße 2, 30419 Hannover, Germany; dierks@cell.uni-hannover.de; lehrich@cell.uni-hannover.de

[2] Université Paul Sabatier, Toulouse III, UMR 5068, Laboratoire de Synthèse et Physicochimie des Molécules d'Intérêt Biologique, 118 Route de Narbonne, F-31062 Toulouse Cedex 9, France

[3] CNRS, UMR 5068, Laboratoire de Synthèse et Physicochimie des Molécules d'Intérêt Biologique, 118 Route de Narbonne, F-31062 Toulouse Cedex 9, France; florence.bedos@univ-tlse3.fr

[4] Center for Systems Neuroscience (ZSN), University of Veterinary Medicine Hannover Foundation, Bünteweg 2, 30559 Hannover, Germany

* Correspondence: ngezahayo@cell.uni-hannover.de; Tel.: +49 511 762 4568

Abstract: Inflammation mediators enhance the activity of connexin (Cx) hemichannels especially in the epithelial and endothelial tissues. As potential release route for injury signals like (oligo)nucleotides, Cx hemichannels may contribute to long lasting inflammation. Specific inhibition of Cx hemichannels may therefore be a mode of prevention and treatment of long lasting, chronic sterile inflammation. The activity of Cx hemichannels was analysed in N2A and HeLa cells transfected with human Cx26 and Cx46 as well as in Calu-3 cells using the dye uptake as functional assay. Moreover, possible impact of the bioactive phenolic agents CVB2-61 and CVB4-57 on the barrier function of epithelial cells was analysed using Calu-3 cells. Both agents inhibited the dye uptake in N2A cells expressing Cx26 (> 5 μM) and Cx46 (> 20 μM). In Calu-3 cells, CVB2-61 and CVB4-57 reversible inhibited the dye uptake at concentrations as low as 5 μM, without affecting the gap junction communication and barrier function, even at concentrations of 20 μM. While CVB2-61 or CVB4-57 maintained a reduced dye uptake in Calu-3 cells, an enhancement of the dye uptake in response to stimulation of adenosine signaling was still observed after removal of the agents. The report shows that CVB2-61 and CVB4-57 reversible block Cx hemichannels. Deciphering the interaction mechanisms with Cx hemichannels could allow further development of phenolic compounds to target Cx hemichannels for a better and safer use in treatment of pathologies that involve Cx hemichannels.

Keywords: connexin channels; inflammation signals; dye uptake; transepithelial electrical resistance (TEER); polyphenols; curcuminoids; Calu-3 cells

1. Introduction

Connexins (Cx) are membrane proteins whose most recognized function is the formation of gap junction channels that directly connect the cytoplasmic spaces of adjacent cells in tissue [1], [2]. The Cx gap junction channels are large enough to allow exchange of ions and metabolites such as (oligo)nucleotides and peptides up to 1.5 kDa [1], [3]. Cxs also form unapposed hemichannels in the membrane of individual cells [2]. In most tissues, the activity of the Cx hemichannels is maintained very low by the docking between adjacent cells that reduces the density of unapposed Cx hemichannels. Moreover, the interstitial Ca^{2+} concentration of about 2 mM strongly reduces the open probability of Cx hemichannels [4]. Due to their large pores, Cx hemichannels allow the influx of solutes from the extracellular milieu as well as the release of intracellular molecules which may act as injury signals in the tissue [2].

 doi:10.20944/preprints202209.0120.v1

Increased activity of Cx hemichannels has been involved in inflammation, the hallmark of various pathologies like atherosclerosis, neurodegenerative diseases, respiratory stress, and genetic-related disorders in different organs as well as the age related disabilities commonly referred as inflamm-aging [5], [6], [7], [8], [9]. Cx hemichannels have also been involved in tumour development [10]. The mechanisms that lead to the increased activity of Cx hemichannels under the mentioned pathological conditions are still matter of ongoing research. Due to experimental convenience, an increased expression of mainly Cx43 has been extensively reported [11], [12], [13]. Likewise, the link between the activity of Cx hemichannels and the pathological status is still poorly understood. For tumours, a role of Cx hemichannels as release route for anti-oxidant [14] and survival mediators, like bisphosphates [15], has been proposed. In the case of inflammation, the enhancement of Cx hemichannels and a resulting increased release of injury signals like (oligo) nucleotides that may continue to trigger inflammation even after infection decay or injury repair is one of the hypothesis that are constantly proposed [16], [17]. In addition to the clarification of the mechanisms leading to the increased activity of Cx hemichannels, there is considerable research aiming the development of agents that block Cx hemichannels to prevent or treat various diseases [18]. Different properties would be expected for an ideal blocker: (i) to target selectively the Cx hemichannels and not the gap junction channels, (ii) to be isoform specific and (iii) to not alter the tissue physiology.

Inflammation is a response to invader microbes and substances released from them commonly known as pathogen-associated molecular patterns (PAMPs). Inflammation is also triggered when a tissue is injured. In this latter case, injured cells release in tissue intracellular molecules such as nucleotides, known as tissue injury signals, commonly called damage-associated molecular patterns (DAMPs) [19]. The invading microorganisms and their released PAMPs after binding to so called toll-like receptor (TLR) in cell membranes, mainly of epithelial cells. They may induce injury-like response in epithelial cells, resulting in the release of DAMPs and the activation of cytokine synthesis and secretion [20]. The released DAMPs and cytokines can act as chemoattractants and chemostimulants for immune cells that trigger inflammation as a starting point for removal of the invader or injury healing [21].

Enhancement of the activity of Cx hemichannels in epithelial cells in response to PAMPs and DAMPs as recently shown [12], [22] may correlate with an increased release of injury signals during inflammatory events. An increased and possible persistent enhancement of Cx hemichannels may therefore represent a detrimental response of epithelial cells to invaders and PAMPs that would continue to release DAMPs even after the decay of infection.

Polyphenols and curcuminoids are known for their anti-inflammatory activity [23]. These natural products found in food and beverages as well as in nutrient complements, present low toxicity and are currently tested in clinical usage mostly as complement for other anti-inflammation pharmaceutics [24], [25]. In animal model, polyphenols and curcuminoids inhibit the reactive oxygen species production or the expression and release of inflammatory cytokines by innate immune system cells [26], [27], [28]. Although these natural products exhibit poor pharmacokinetic properties, they represent a good starting point for the design of biological active agents. In the present article, we report the study of CVB2-61, a phenolic diarylether, which is a dimer of a vanillin derivate with antiatherogenic properties [6] and CVB4-57, a diarylheptanoid and a curcuminoid analogue, as specific agents to target Cx hemichannels.

2. Results

2.1. Synthesis of the bioactive phenolic agents CVB2-61 and CVB4-57

CVB2-61 (Figure 1a) was synthesised as previously described [29]. CVB4-57 was obtained in three synthesis steps starting from piperazine, involving two successive N-alkylation of with (4-(2-bromoethyl)phenoxy)(tert-butyl)dimethylsilane and 2-bromo-4-

Preprints (www.preprints.org) | NOT PEER-REVIEWED | Posted: 8 September 2022 doi:10.20944/preprints202209.0120.v1

(bromomethyl)-1-methoxybenzene followed by tetrabutylammonium fluoride (TBAF) deprotection of the phenol group as depicted in figure 1b.

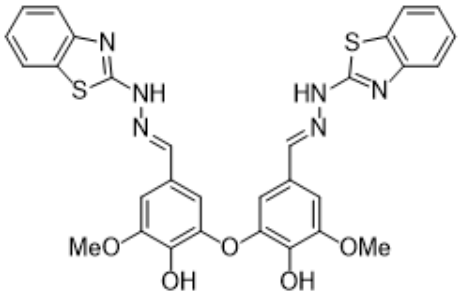

(**a**)

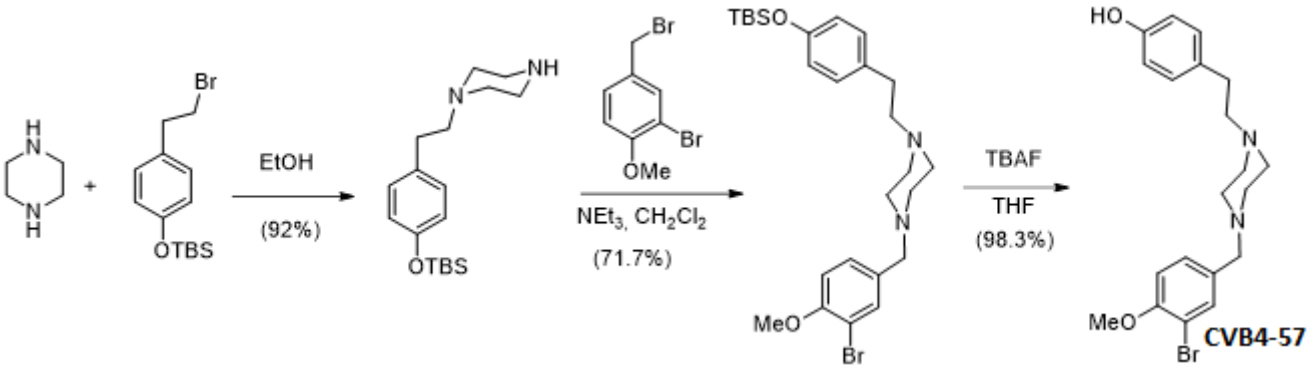

(**b**)

Figure 1. Chemical structure of the studied bioactive phenolic agents. (**a**) CVB2-61, was synthesized as previously described [29] and (**b**) CVB4-57 that was synthesized in three steps as depicted.

2.2. Connexin expression in N2A and HeLa cells

Molecular cloning was used to generate IRES vectors containing the DNA sequence of the Cx isoform Cx26 or Cx46 and GFP. We used these two Cx isoforms for their known function/ability to form Cx hemichannels *in vivo* in tissues like the ocular lens, skin and the inner ear [30], [31]. Additionally a crystal structure model of Cx26 [32] is available and gives valuable information for further analysis and simulation processes [33] in common studies of the interaction mechanisms of the compounds with Cx hemichannels. The constructs were expressed in N2A and HeLa cells (Figure S1) that do no express endogenous Cxs, to analyse their capacity to form Cx channels. The IRES vector allowed a concomitant expression of GFP and Cxs. However, these two proteins are not linked together. The presence of GFP in the cytoplasmic space was used as control for a successful transfection and expression of the Cxs but did not interfere with the Cx channels functionality. Confocal laser scanning microscopy showed a reliable expression of the proteins in the cells with a transfection efficiency of about 35%. A similar transfection efficiency was also observed in cells transfected with a vector containing only the GFP gene (Figure S1). These latter were used as control in further analysis of the functionality of the Cx hemichannels. Expression of the Cxs was further verified by immunofluorescence staining (Figure S1). As shown in figure S1, the Cxs were expressed and exported to the cell membrane. In some cells, Cx associations were found at the cell-to-cell contact and the cell border (Figure S1;

 doi:10.20944/preprints202209.0120.v1

red arrows), where they presumably formed cell-to-cell gap junction channels or Cx hemichannels. In other cells, a cytoplasmic localization probably in the endoplasmic reticulum (ER) and Golgi apparatus of the Cxs was observed (Figure S1; white arrows).

2.3. Functionality of expressed Cx hemichannels

In order to analyse the functionality of the formed Cx hemichannels in the membrane of transfected cells, we performed dye uptake experiments [11], [34], [35], [36]. The functionality of Cx hemichannels was recognized as an accelerated increase of fluorescence intensity of the dye ethidium bromide (Etd) in the cells in response to the removal of external Ca^{2+} as compared to control conditions with 2 mM external Ca^{2+} (Figure 2a). The rate of dye uptake was quantified to compare cells expressing the Cx variants with cells expressing GFP alone. The fluorescence intensity of Etd was measured in the cells and plotted vs time when cells were incubated with or without external Ca^{2+}. A linear regression was applied on the measured curve. The rate of dye uptake in presence or absence of external Ca^{2+} was estimated as the slope of the linear regression in Ca^{2+}-containing and Ca^{2+}-free sectors of the experiment (Figure 2a). The rate of dye uptake in cells expressing the Cx variants and those expressing GFP alone was low when external Ca^{2+} (2 mM) was present. The removal of external Ca^{2+} showed an increased rate of dye uptake in cells expressing the Cx variants compared to cells expressing GFP alone (Figure 2b, Figure S2b). It is worth to note that the dye uptake rate in cells expressing GFP without Cx variants was similar to that measured in non-transfected cells (Figure S2a). As shown in Figure 2b, the rate of Etd uptake in cells expressing Cx variants together with GFP was significantly higher compared to that estimated in cells expressing GFP alone, with 3.1 ± 0.4 fold of hCx26 ($p < 0.001$) and 4.1 ± 0.5 fold of hCx46 ($p < 0.001$) in N2A cells (Figure 2b; for HeLa cells: Figure S2b). This observation gives evidence that even if the open probability of the hemichannels was reduced by external Ca^{2+}, a presence of Cx hemichannels in the membrane allowed an uptake of Etd in the N2A cells, that was significant higher in cells expressing Cxs compared to cells expressing GFP alone (Figure 2b). The N2A cells expressing the respective Cx give a good basis to test the capacity of different compounds to inhibit Cx hemichannel activity.

2.4. Inhibition of Cx hemichannels

CVB2-61 and CVB4-57 were tested on cells expressing hCx26 and hCx46 (Figure 3; Figure S3). In presence of 5 μM CBV2-61, the dye uptake in cells expressing hCx26 decreased to 60 ± 6%. An increase in the CBV2-61 concentration to 20 μM did not result in a significant increase in the effect. However, the statistical significance of the reduction of the dye uptake rate ($p < 0.05$ for 5 μM; $p < 0.01$ for 10 μM; $p < 0.001$ for 20 μM) was strengthened in comparison to the control experiment without CVB2-61 (Figure 3a). For CVB4-57, a significant reduction of the dye uptake rate (79 ± 17%) was already observed at 1 μM ($p < 0.05$) in cells expressing hCx26 (Figure 3b). Increasing the concentration to 5 μM reinforced the reduction to 50 ± 12% ($p < 0.01$). A further increase of the CVB4-57 to 20 μM induced a further reduction of the dye uptake rate (34 ± 2%, $p < 0.001$) (Figure 3b). In N2A cells expressing Cx46, a reduction of the dye uptake about 72 ± 3% ($p < 0.001$) was only observed at the high concentration of 20 μM for both CVB2-61 and CVB4-57 (Figure 3c, d).

Preprints (www.preprints.org) | NOT PEER-REVIEWED | Posted: 8 September 2022 doi:10.20944/preprints202209.0120.v1

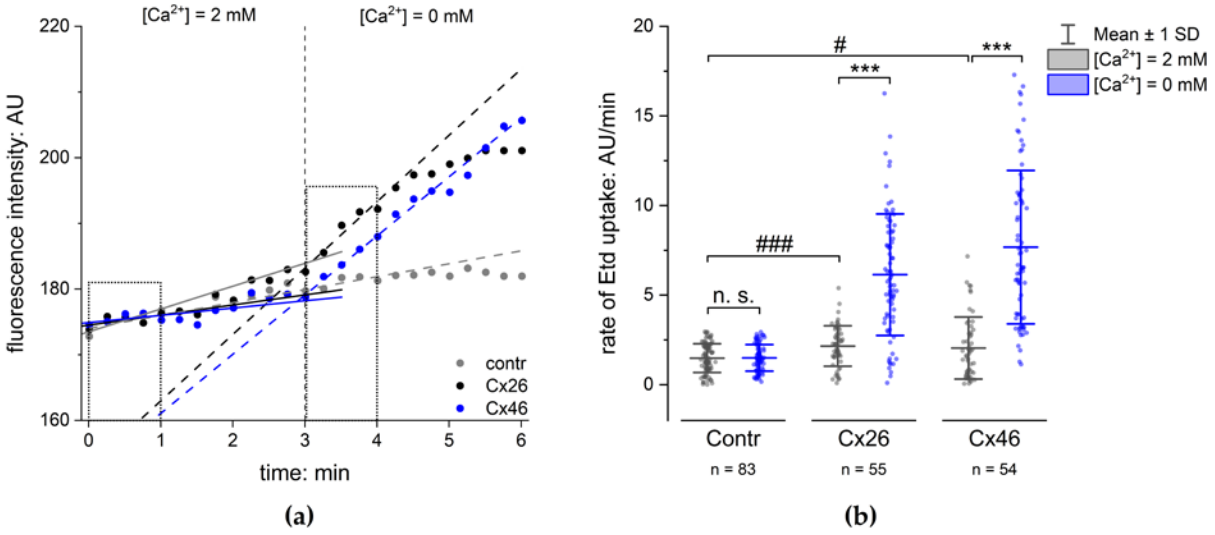

Figure 2. Dye uptake in N2A cells expressing connexins. (**a**) The time course of the fluorescence intensity of Etd in N2A cells transfected with GFP vector (Contr), hCx26IRES-GFP (Cx26) vector or Cx46IRES-GFP vector (Cx46). The dots show the fluorescence intensity measured in single cells expressing only GFP (grey), Cx26 (black) and Cx46 (blue) in presence and absence of external Ca^{2+}. Removal of external Ca^{2+} led to a rapid increase of the measured fluorescence intensity in the cells expressing Cxs, but not in the control cells, indicating an opening of the Cx hemichannels. The lines show a linear regression along the fluorescence intensity in presence and absence of external Ca^{2+}, the slope was used to estimate the rate of Etd uptake. (**b**) Rate of Etd uptake in N2A cells transfected with the Cx isoforms compared to cells expressing GFP alone (Contr). The results are given as mean ± SD of at least three respective transfections. The number of analysed cells is given as n. One-way ANOVA was applied to estimate the statistical significance (p: # < 0.05; ***, ### < 0.001).

Additionally to N2A cells, we studied the effect of CVB2-61 and CVB4-57 on Cx channels in Calu-3 cells. In contrast to N2A cells, Calu-3 cells endogenously express Cxs. Calu-3 cells are epithelial cells of the human respiratory airways forming a good barrier *in vitro* [37] and are therefore considered as an adequate model to investigate physiological functions of the lung epithelium [11], [38], as well as for development of therapeutics for various lung diseases [39]. The ability of CVB2-61 and CBV4-57 to inhibit Cx hemichannels in Calu-3 cells was studied (Figure 4, Figure S4) in reference to previously published results, showing that inflammatory signals like adenosine enhanced the activity of Cx26 hemichannels in Calu-3 cells [11]. CVB2-61 or CVB4-57 (5 µM) was added to the cells at the same time as the removal of external Ca^{2+}. An inhibition of the dye uptake was then noticed (Figure 4, Figure S4). This effect was observed in cells that were cultivated for 24 h in presence of the adenosine analogue 5-N-Ethylcarboxamidoadenosine (NECA) as well as in cells cultivated under control conditions (Figure 4, Figure S4). The repression of the dye uptake was due to the presence of CVB2-61 and CVB4-57, since the removal of the agents during the dye uptake experiments correlated with an immediate acceleration of the dye uptake rate. In addition, the enhanced rate of dye uptake related to cultivation of the cells under stimulation of adenosine receptors using NECA was still observable after removing of the compounds CVB2-61 and CVB4-57 (Figure 4, Figure S4).

Preprints (www.preprints.org) | NOT PEER-REVIEWED | Posted: 8 September 2022 doi:10.20944/preprints202209.0120.v1

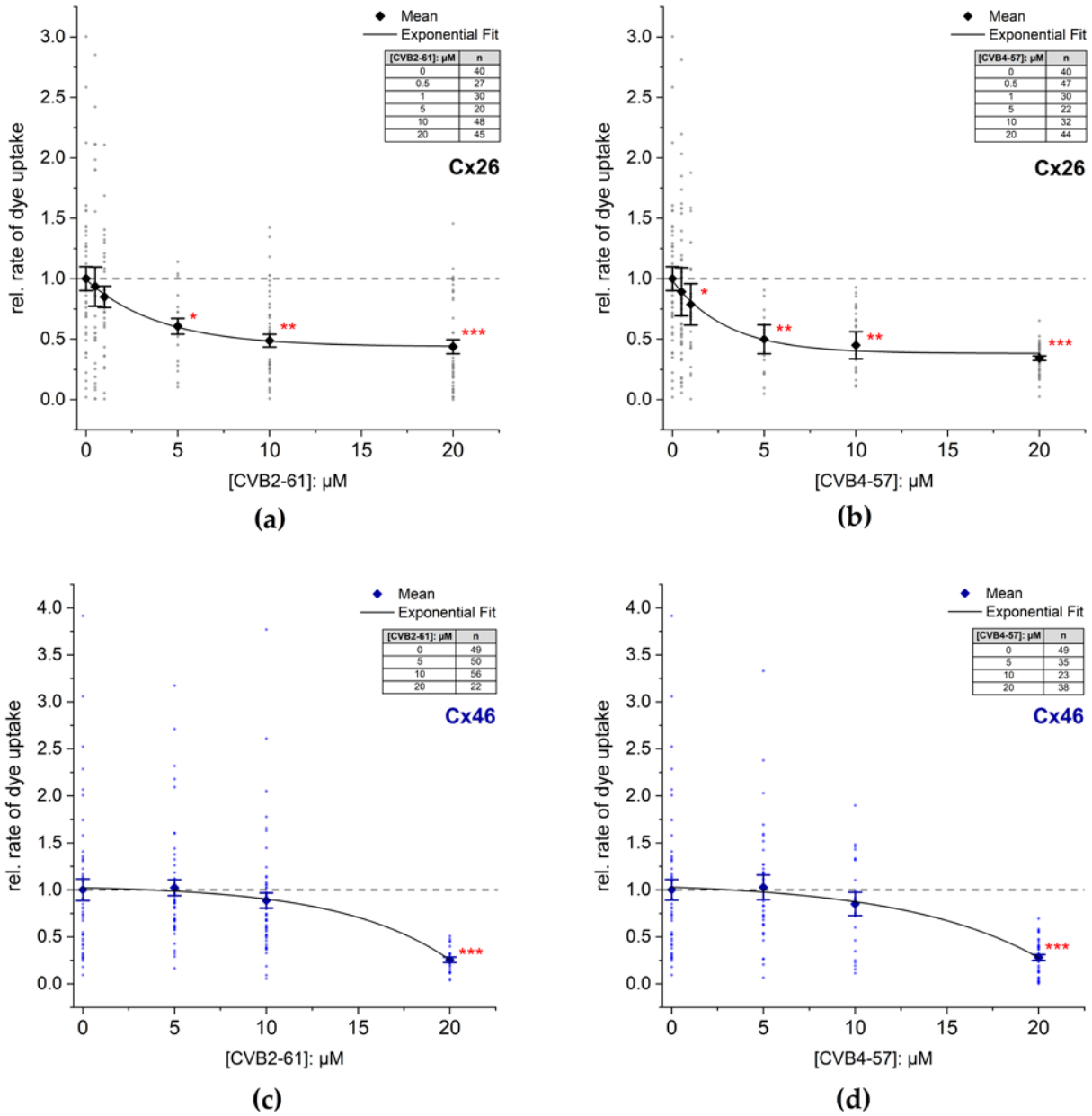

Figure 3. Inhibition of dye uptake by the agents CVB2-61 or CVB4-57. The rate of dye uptake in Cx26 (**a, b**) or Cx46 (**c, d**) expressing N2A cells was measured in Ca^{2+} free external solution in presence or absence of the indicated concentrations of CVB2-61 (**a, c**) and CVB4-57 (**b, d**). Representative experiments indicating the time course of the dye uptake in presence of the compounds are given in figure S3. The data were normalised to the mean rate of dye uptake found in N2A cells expressing Cxs after removal of external Ca^{2+} and in absence of the agents. The data are given as mean ± SEM for at least three respective transfections. The number of cells used for each experiment is given as n. The lines were obtained by fitting the means to a single exponential function. One-way ANOVA was applied to estimate the statistical significance to the 0 µM treated cells (p: * < 0.05; ** < 0.01; *** < 0.001).

The above presented results show that when applied for the short period of the dye uptake experiment, the response of Calu-3 cells did not differ between the compounds CVB2-61 and CVB4-57. When applied for a long application period (24 h) the response induced by CVB2-61 slightly differed from that induced by CVB4-57. In cells cultivated in presence of CVB2-61, the increase of the dye uptake rate observed after suppression of

Preprints (www.preprints.org) | NOT PEER-REVIEWED | Posted: 8 September 2022 doi:10.20944/preprints202209.0120.v1

both external Ca^{2+} and CVB2-61 was reinforced compared to cells cultivated under control conditions (Figure 4a, Figure S4). An additional enhancement was further observed in cells cultivated in presence of CVB2-61 and NECA (Figure 4a, Figure S4). In contrast, for cells cultivated in presence of CVB4-57, the increase was similar to that found in cells cultivated under control conditions (Figure 4b). Correspondingly the enhancement of the dye uptake rate due to NECA was not affected by the presence of the CVB4-57 during the cultivation compared to cells cultivated without CVB4-57 and in presence of NECA (Figure 4b). These different effects of CVB2-61 and CVB4-57 should be exploited to further study how they block Cx hemichannels and their overall effects in the cell.

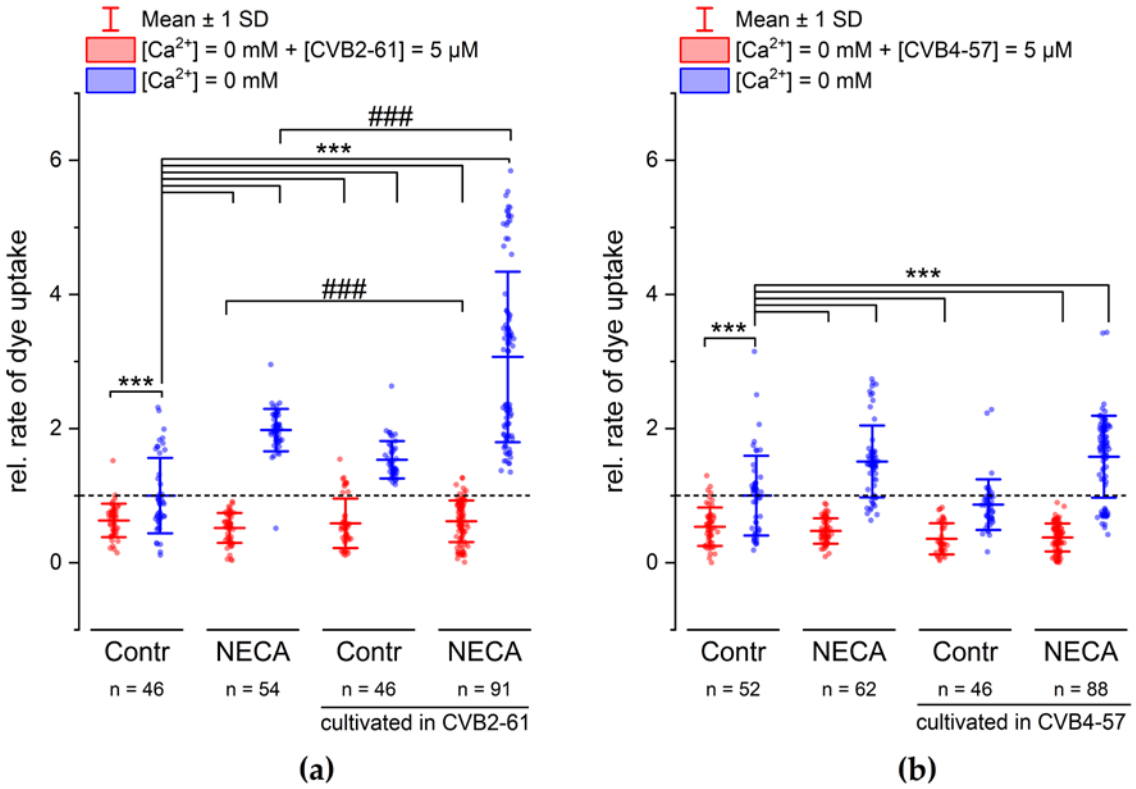

Figure 4. CVB2-61 and CVB4-57 inhibited the dye uptake in Calu-3 cells. The effect of the compounds (5µM) (**a**) CVB2-61 or (**b**) CVB4-57 on the rate of dye uptake after removing of external Ca^{2+}. When applied for the short period of the dye uptake assay, both CVB2-61 and CVB4-57 maintained the dye uptake rate reduced in cells cultivated under control conditions and those cultivated in presence of NECA (24 h, 10 µM). The removing of CVB2-61 or CVB4-57 was followed by an increased dye uptake rate. Note the enhanced dye uptake rate observed in cells cultivated in the presence of NECA was similar to recently published results [11]. For cells cultivated with the compounds for 24 h, modifications of the dye uptake rate were only observed for CVB2-61. Cells cultivated with CVB2-61 showed a significant enhanced dye uptake rate compared to cells cultivated under control conditions (Contr). Correspondingly cells cultivated with CVB2-61 and NECA showed a more enhanced dye uptake rate compared to cells cultivated with NECA alone. The data were normalised to the mean of the rate of dye uptake observed in cells cultivated under control conditions (Contr, blue box plot). The data are given as mean ± SD of at least three biological replicates, n indicates the number of analysed cell patches. A cell patch contained 5-40 cells. One-way ANOVA was applied to estimate the statistical significance (p: ***, ### < 0.001).

Many Cx channel inhibitors such as glycyrrhetinic acid (GA) and its derivate carbenoxolone (CBX) affect both the Cx hemichannels and the gap junction channels [41]. In addition, it was shown that GA affected the barrier function of epithelial cells [42]. Our data also show that CBX altered the barrier function at concentrations commonly used to

Preprints (www.preprints.org) | NOT PEER-REVIEWED | Posted: 8 September 2022 doi:10.20944/preprints202209.0120.v1

block Cx channels (Figure 5a). In contrast, we found that both CVB2-61 and CVB4-57 did not alter the barrier function of Calu-3 monolayers cultivated in transwell inserts shown by measuring the transepithelial electrical resistance (TEER) by impedance spectroscopy (Figure 5a). Moreover, the agents inhibited the dye uptake, meaning they blocked the Cx hemichannels without altering the gap junction related dye transfer. Using the gold nanoparticle mediated laser perforation/ dye transfer (GNOME-LP/DT) method as described previously [11], [40], we found that both agents did not affect the degree of gap junction coupling, neither when applied spontaneously nor when applied during cultivation for 24 h (Figure 5b). Taken together the above reported results suggest that CVB2-61 and CVB4-57 could block Cx hemichannels with minimal impact on the epithelial physiology.

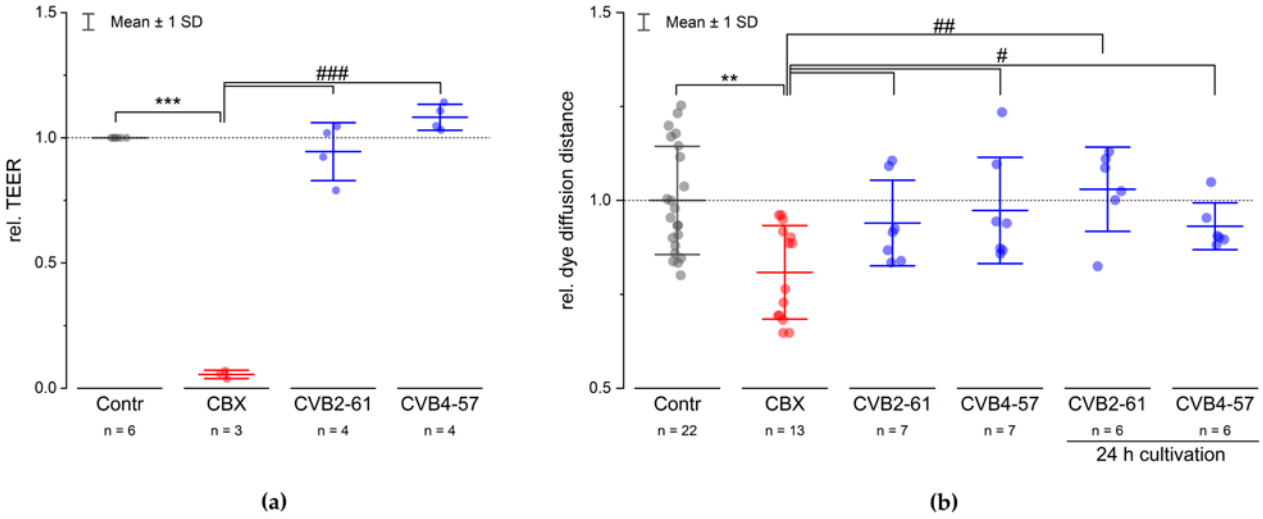

Figure 5. The CVB2-61 and CVB4-57 did not affect the barrier function or gap junction communication. (**a**) The effect of CVB2-61 (20 µM) and CVB4-57 (20 µM) on the TEER of Calu-3 cells cultivated in transwell inserts with a TEER value of at least 1000 Ωcm² is shown. (**b**) The dye diffusion distance in Calu-3 cells monolayer as estimated by the gold nanoparticle mediated laser perforation/ dye transfer method (GNOMELP/ DT; [43]) in presence or absence of CVB2-61 (20 µM) and CVB4-57 (20 µM). Compared to control cells, the compounds CVB2-61 and CVB4-57 did not change neither the TEER value nor the dye diffusion distance. Of note even if the compounds were already present in the cells during a cultivation time of 24 h, the dye diffusion distance was not affected. In contrast CBX (100 µM) a commonly used inhibitor of Cx channels strongly reduced the TEER (**a**) and, as expected, the dye diffusion distance (**b**). The data were normalized to the mean of the results found in the corresponding control cells and are given as mean ± SD of at least three respective experiments, n indicates the number technical replicates. One-way ANOVA was applied to estimate the statistical significance (p: ***, ### < 0.001; **, ## < 0.01; # < 0.05).

In summary, the present study shows that the agents CVB2-61 and CVB4-57 are able to reversible block Cx hemichannels in a Cx expression system as well as in native cells without affecting the activity of the gap junction channels. In comparison, Cx26 hemichannels are more sensitive to both agents compared to Cx46.

3. Discussion

Evidence has accumulated showing that inflammation inducers like the lipopolysaccharide (LPS) of gram negative bacteria, or injury signals like adenosine enhanced the activity of Cx hemichannels in different tissues especially the epithelial one [11], [12], [13]. Since hemichannels are permeable to molecules that act as injury signals, the enhancement of activity of Cx hemichannels may represent a detrimental response of cells to inflammation inducers. They may start and sustain a long lasting inflammation that persist after the

 doi:10.20944/preprints202209.0120.v1

infection decay with the risk to become a chronic sterile inflammation [6], [13], the hallmarks of various but unrelated pathological situations like chronic obstructive pulmonary disease (COPD) or asthma in the respiratory system [43], or neurological degenerative diseases [6]. It was therefore proposed that compounds able to block the hemichannels could be used for the prevention and treatment of these different pathologies [18]. As Cx hemichannels are also involved in cancer development [10], inhibitors of Cx hemichannels could be of interest for cancer therapy [44]. Finally, for a low general toxicity, the ideal compound should target the Cx hemichannels specifically without affecting the gap junction channels or altering the tissue physiology.

So far, different small molecules, such as the antimalarial agents like quinine and mefloquine, the non-steroidal anti-inflammatory drug like fenamates; the anesthetic drugs like propofol and ketamine; glycyrrhetinic acid (GA) and its derivatives like carbenoxolone (CBX); alcohols like heptanol and octanol; 2-aminoethoxydiphenyl borate, mimetic peptides of Cx extracellular loops sequences as well as anti-Cx antibodies and aminoglycoside antibiotics and their derivatives, without antibiotic effects have been tested to block Cx hemichannels. Many small molecules and mimetic peptides mentioned above as well as anti-Cx antibodies, poorly distinguished gap junction channels from Cx hemichannels [45], [46]. However, the small molecule boldine [47] and the mimetic peptide Gap19 [48] as well as the aminoglycoside antibiotics [49], [50] were shown to block Cx43 hemichannels. The mimetic peptide Gap19, designed on the basis of the Cx43 intracellular loop sequence needs to enter the cells to function. Boldine is an alkaloid tested on Cx43 that may function without entering into the cells. Considering the antibodies, a potent anti-Cx26 antibody capable to block Cx26 hemichannels without affecting the gap junction channels was generated [51]. With respect to antibiotics, a derivative of kanamycin A, the compound 12i showed a selectivity to Cx43 hemichannels compared to Cx26 hemichannels [50], [52]. The mentioned anti-Cx26 antibody, the Gap19 mimetic peptide and the small molecule boldine as well as the antibiotics derivatives show the undergoing development of compounds capable of specifically inhibiting Cx hemichannels. In the present report, we studied two agents CVB2-61 and CVB4-57 which are able to reversible block human Cx hemichannels in an expression system as well as in native cells (Figure 3, Figure 4). In Calu-3 cells (human lung epithelial cells), which are naturally expressing Cx [11], the two agents were found to not affect the gap junction coupling (Figure 5b) suggesting that they may specifically target the Cx hemichannels. Moreover, Cx26 hemichannels were already inhibited at a concentration of agents as low as 5 μM, while a higher concentration (20 μM) was needed to inhibit Cx46 hemichannels (Figure 3). Finally, the two agents do not appear to alter the barrier function of the epithelial cells as important physiological character of the epithelium (Figure 5a).

CVB2-61 [29], is a dimer constituted by two benzothiazole-vanillin units linked together by an ether oxide bridge (Figure 1a). Due to its antioxidant, antiradical and antiangiogenic properties, CVB2-61 is a good drug-candidate to prevent atherosclerosis [29]. CVB4-57 is an original analogue of curcuminoids, which are known for their anti-inflammatory properties [53], [54]. CVB4-57 exhibits a phenolic moiety, which may confer its radical quenching properties [55]. A piperazine core was inserted between the two aromatic moieties to replace heptanoid chain, to ensure rigidity to CVB4-57 and finally to add two nitrogen atoms for potential H-bond interactions with Cx amino acids (Figure 1b). Since piperazine has a well-known pharmacophore [37], a low cytotoxicity for CVB4-57 can be expected.

The data presented here show that both CVB2-61 and CVB4-57, at the used concentrations, may selectively affect the Cx hemichannels without disturbing the Cx gap junction channels neither in the opened nor in the closed formation (Figure 5b). Moreover, Cx26 was found to be more sensitive to the agents than Cx46 (Figure 3) suggesting that a Cx isoform specificity may be achieved. Furthermore, in Calu-3 cells treated simultaneously with the respective agent and the adenosine receptor agonist NECA for 24 hours,

 doi:10.20944/preprints202209.0120.v1

both agents maintained a reduced dye uptake rate. After their removal from the cells during the experiments, the activity of the hemichannels was released and the NECA-induced enhancement of the rate of dye uptake [11] was still observed compared to cells cultivated under control conditions (Figure 4). The NECA related enhancement of the dye uptake rate was shown to be linked to an increased expression of Cx26 [11]. We therefore assume that CVB2-61 and CVB4-57 did not negatively interfere with gene expression e.g. the expression of Cx26.

The action mechanisms of the agents CVB2-61 and CVB4-57 affecting the Cx hemichannels are not yet elucidated. For small molecules such as long chain alcohols and anaesthetics that inhibit Cx channels, an indirect effect due to induced changes in membrane fluidity has been proposed [56], [57], [58]. This may explain why these small molecules and anaesthetics do not distinguish the gap junction channels and the Cx hemichannels. Likewise, these small molecules and anaesthetics are not expected to achieve any isoform specificity. Since the gap junction channels were not affected by neither CVB2-61 nor CVB4-57 (Figure 5b), a similar model of action to that proposed for alcohols or anaesthetics seems unlikely. Finally, some small molecules may have detrimental effects on the physiology of tissue as revealed by the observation that GA [42] and CBX affected the barrier function (Figure 5a). The mimetic peptides such as Gap26, Gap27 [59] or many anti-Cx antibodies bind extracellular domains of the Cx and thus probably interfere with Cx hemichannel opening. Many small molecules as well as mimetic peptides or antibodies do not only affect the Cx hemichannels. Depending on the duration of the application they have a negative impact on the gap junction channels. These effect on gap junction channels is spontaneous and reversible for the small molecules [45]. For mimetic peptides as well as antibodies, the effects are slow and may be related to the competition of mimetic peptides or antibodies with the docking mechanism of Cx hemichannels. With regards to the Cx isoform specificity, many anti-Cx antibodies used to close the hemichannels are mainly directed against the extracellular domains of the Cxs [45]. Similarly, many mimetic peptides were designed according to the extracellular domains of the Cxs [59]. The extracellular loops of Cxs are short and largely conserved between the Cx isoforms. In this context, the development of Cx isoform specific antibodies as well as mimetic peptides may be challenging. However as shown by Xu et al. 2017 it is possible to develop an anti-Cx26 antibody capable of inhibiting only Cx26 [51]. Furthermore, as shown for Gap19 [48], other more specific regions of the Cx protein distinct from the extracellular domains could be considered for the design of mimetic peptides thus allowing a better Cx-isoform specificity. The agents CVB2-61 and CVB4-57 reversible inhibited the Cx hemichannel opening and did not affect the gap junction channels when applied for 24 h (Figure 5b). These results suggest that both CVB2-61 and CVB4-7 blocked the Cx hemichannels without competing with the docking of Cx hemichannels between adjacent cells. Understanding the mode of interaction between both CVB2-61 or CVB4-57 and the Cx hemichannels still needs clarification involving experiments far above the scope of the present report like crystallization of Cx hemichannels in presence of either agents. Finally, neither CVB2-61 nor CVB4-57 were observed to affect the barrier function of Calu-3 cells (Figure 5a), suggesting that the two compounds are non-cytotoxic. Moreover, these two small molecules may be less recognized by the immunological system. These last two aspects will offer an obvious advantage to use them as tools to study the role of Cx hemichannels in function of epithelial barrier in order to develop drugs to treat diseases involving Cx hemichannels.

4. Materials and Methods

4.1. Chemical synthesis of the bioactive agent CVB4-57

4.1.1. *General*

Unless otherwise noted, all experiments were carried out under a nitrogen atmosphere. Solvents (CH_2Cl_2 and THF) were dried *via* a purification solvent system MB-SP-

 doi:10.20944/preprints202209.0120.v1

800 (MBRAUN). Melting points (mp) were obtained on a Buchi apparatus and are uncorrected. IR spectra were recorded on a Thermo Nicolet Nexus spectrometer. NMR spectra were recorded on Brucker Avance 300 MHz spectrometers. The NMR spectra were acquired in $CDCl_3$, and the chemical shifts were reported in parts per million referring to $CHCl_3$ (δ_H 7.26 for proton and δ_C 77.16 for carbon). Signals are described as follow: s, singlet; brs, broad signal; d, doublet; t, triplet; m, multiplet. HRMS data were recorded on a Xevo G2 QTOF (Waters) instrument. Reactions were monitored by TLC on silica gel Alugram® Xtra SIL G/UV$_{254}$. Column chromatography were performed on Machery-Nagel silica gel 0.063-0.2 mm.

4.1.2. *1-(4-((tert-butyldimethylsilyl)oxy)phenethyl)piperazine*

To a mixture of piperazine (1.36 g, 15.86 mmol) in EtOH (5mL) at 70°C was added dropwise a solution of (4-(2-bromoethyl)phenoxy)(tert-butyl)dimethylsilane (500 mg, 1.58 mmol) in EtOH (5 mL). The reaction mixture was stirred at 70°C for 4h. After cooling to room temperature, saturated aqueous NaCl solution was added. The aqueous layer was extracted with $CHCl_3$ and the combined organic layers washed with brine (4x), dried over $MgSO_4$ and concentrated under reduced pressure, yielding to the expected compound (469 mg, 92.7%) as a light yellow oil, which was pure enough to be used in the next step.^{1}H NMR (300 MHz, $CDCl_3$) δ 7.07 – 7.00 (m, 2H), 6.74 (d, *J* = 8.5 Hz, 2H), 3.04 – 2.86 (m, 4H), 2.78 – 2.70 (m, 2H), 2.60 – 2.45 (m, 6H), 0.97 (s, 9H), 0.17 (s, 6H). ^{13}C NMR (75 MHz, $CDCl_3$) δ 153.7, 132.8, 129.4, 119.8, 61.2, 54.2, 45.8, 32.4, 25.6, 18.0, -4.5.

4.1.3. *1-(3-bromo-4-methoxybenzyl)-4-(4-((tert-butyldimethylsilyl)oxy)phenethyl)piperazine*

To a solution of piperazine derivative **1** (469 mg, 1.46 mmol) in CH_2Cl_2 (15 mL) were added NEt_3 (0.3 mL, 2.2 mmol) and 2-bromo-4-(bromomethyl)-1-methoxybenzene (430 mg, 3.54 mmol). The reaction mixture was stirred at room temperature overnight. Then water was added and the aqueous layer was extracted with CH_2Cl_2. The combined organic layers were washed with brine, dried over $MgSO_4$ and concentrated under reduced pressure. The crude product was purified by silica gel column chromatography (CH_2Cl_2 to CH_2Cl_2/MeOH = 98:2) to provide compound **2** as a colorless oil (545 mg, 71.7%). ^{1}H NMR (300 MHz, $CDCl_3$) δ 7.52 (d, *J* = 2.1 Hz, 1H), 7.21 (dd, *J* = 8.4, 2.1 Hz, 1H), 7.08 – 7.00 (m, 2H), 6.84 (d, *J* = 8.4 Hz, 1H), 6.78 – 6.71 (m, 2H), 3.88 (s, 3H), 3.43 (s, 2H), 2.80 – 2.37 (m, 12H), 0.97 (s, 9H), 0.17 (s, 6H). ^{13}C NMR (75 MHz, $CDCl_3$) δ 154.8, 153.7, 133.8, 129.5, 129.1, 119.8, 111.5, 111.4, 77.2, 61.7, 60.6, 56.2, 53.1, 52.9, 32.8, 25.7, 18.1, -4.5. HRMS (DCI-CH_4) *m/z* for $C_{26}H_{40}N_2O_2SiBr$ $[M+H]^+$ Calcd: 519.2042, Found: 519.2016.

4.1.4. *4-(2-(4-(3-bromo-4-methoxybenzyl)piperazin-1-yl)ethyl)phenol: CVB4-57*

To an ice-cooled solution of compound **2** (545 mg, 1.05 mmol) in anhydrous THF (15 mL) was added dropwise *n*-Bu_4NF solution (1M in THF, 2.1 mL, 2.1 mmol). The reaction mixture was stirred at 0°C for 4h. Saturated aqueous $NaHCO_3$ solution was added and the aqueous layer was extracted with EtOAc. The combined organic layers were washed with saturated aqueous $NaHCO_3$, water and brine, dried over $MgSO_4$ and concentrated under reduced pressure. The crude product was purified by silica gel column chromatography (CH_2Cl_2 to CH_2Cl_2/MeOH = 95:5) to provide the expected compound as a white solid (418 mg, 98.3%). mp = 151-152°C.^{1}H NMR (300 MHz, $CDCl_3$) δ 7.51 (d, *J* = 2.0 Hz, 1H), 7.20 (dd, *J* = 8.4, 2.1 Hz, 1H), 7.02 (d, *J* = 8.4 Hz, 2H), 6.83 (d, *J* = 8.4 Hz, 1H), 6.70 (d, *J* = 8.4 Hz, 2H), 3.88 (s, 3H), 3.44 (s, 2H), 2.87 – 2.31 (m, 12H). ^{13}C NMR (75 MHz, $CDCl_3$) δ 155.1, 154.8, 134.2, 131.3, 131.2, 129.8, 129.5, 115.8, 111.7, 111.5, 61.8, 60.7, 56.4, 52.9, 52.6, 32.3. HRMS (DCI-CH_4) *m/z* for $C_{20}H_{26}N_2O_2Br$ $[M]^+$ Calcd: 405.1178, Found: 405.1162. IR (KBr): ν = 3522 cm^{-1}.

4.2. Materials

Both CVB2-61 and CVB4-57 were stored at -20 °C and were solved in DMSO and stored at -20 °C used for max. 6 months. Lucifer Yellow and carbenoxolone (CBX) were

 doi:10.20944/preprints202209.0120.v1

purchased from Sigma-Aldrich (Taufkirchen, Germany) and solved in sodium NaCl-bath solution without Ca^{2+} composed as follows (in mM) 145 NaCl, 5.4 KCl, 1 MgCl2, 5 glucose, 10 Hepes (295 mOsmol; pH: 7.4). The vehicles (for the compound CBV2-61 and CBV4-57), DMSO was added to control cells in all experiments at maximal concentrations of 0.1% respectively. Transfection reagent FuGENE® HD was purchased from Promega (Walldorf, Germany) and used according to the transfection protocol.

4.3. Molecular cloning and transfection

For this work the expression vectors pEF1a B1-hCx26-B2-IRES-GFP, pEF1a B1-hCx46-B2-IRES-GFP [34], [60] were used and constructed by gateway cloning. The gene for human connexin (hCx) isoforms hCx26 or hCx46 were cloned in the vector pEF1a which has an IRES element between the gateway cassette and the reporter GFP. pEF-I-GFP GX [61] was a gift from John Brigande (Addgene plasmid # 45443). The Cx gene sequence insert was placed with attB sides, shown in table 1, into a pDONR™ 221 by Gateway BP cloning. By Gateway LR cloning the Cx gene sequence was integrated into the pEF-I-GFP. The constructs (pEF1a B1-hCx26-B2-IRES-GFP, pEF1a B1-hCx46-B2-IRES-GFP) were transformed in competent *Escherichia coli* Mach 1 cells and selected on ampicillin-containing LB, the plasmids were extracted with the QIAprep Spin Miniprep Kit (QUIAGEN) after protocol and controlled by sequencing. As control the peGFP-N1 vector was used with a CMV promoter and a gfp gene sequence.

For transfection of Neuro-2A (N2A) cells (DSMZ no.: ACC 148) and HeLa cells (DSMZ no.: ACC 57) with the hCx26-IRES, hCx46-IRES or the GFP plasmids, the cells were seeded on 5 mm diameter coverslips coated with rat collagen I and cultivated till 40% confluence. The cells were transfected with 0.9 µl FuGene HD and 0.3 µg Plasmid DNA for 24 h in 300 µl cultivating media Dulbecco's MEM/Ham's F-12 medium (Biochrom, Berlin, Germany) supplemented with 10% foetal calf serum (Biochrom, Berlin, Germany), 1 mg/ml penicillin, and 0.1 mg/ml streptomycin (Biochrom, Berlin, Germany)). After 24 h the cells were ready for the experiments.

Table 1. Primers used for the BP-cloning to generate the various entry clones [34].

Primer	5′-3′ sequence
GW_BP-cloning hCx26 attB1 F	GGGGACAAGTTTGTACAAAAAAGCAGGCTTAATGGATTGGGGCACGCT
GW_BP-cl. hCx26 stop attB2 R	GGGACCACTTTGTACAAGAAAGCTGGGTTCTAAACTGGCTTTTTTGACTTCCCAGAAC
GW_BP-cloning hCx46 attB1 F	GGGGACAAGTTTGTACAAAAAAGCAGGCTCCATGGGCGACTGGAGCTTTCTGG
GW_BP-cl. hCx46 stop attB2 R	GGGGACCACTTTGTACAAGAAAGCTGGGTTCTAGATGGCCAAGTCCTCCGGT

4.4. Immunofluorescence staining

The transfected N2A cells or HeLa cells were fixed with an acetone/methanol mix (1:2) for 5 min at -20 °C and blocked with 1% bovine serum albumin (BSA) in phosphate buffered solution (PBS) for 30 min at 37 °C. The primary antibodies Cx46 antibody (1:100, SantaCruz, sc-365394) and Cx26 antibody (1:200, Alomone labs, ACC-212) were diluted in PBS and added to the cells overnight at 4 °C. The secondary iFluor488™-conjugated anti-rabbit and anti-mouse antibodies (AAT Bioquest, 16608, 16528) were diluted 1:1,000 in PBS with 2 µM 4′,6-diamino-2-phenylndole (DAPI) (Sigma-Aldrich) for 1 h at 37 °C. The cells were washed with PBS and stored at 4 °C. The cells we imaged with an Eclipse TE2000-E inverse confocal laser scanning microscope (Nikon GmbH, Düsseldorf, Germany) with a 60 x water immersion objective and the software EZ-C1 (Nikon GmbH).

4.5. Dye uptake assay

The activity of Cx hemichannels was analysed by measuring the Etd uptake. The transfected N2A cells or HeLa cells, as well as the Calu-3 cells (AddexBio no.: C00116001) were cultivated on rat collagen I coated coverslips in Dulbecco's MEM/Ham's F-12 medium (Biochrom, Berlin, Germany) supplemented with 10% foetal calf serum (Biochrom,

 doi:10.20944/preprints202209.0120.v1

Berlin, Germany), 1 mg/ml penicillin, and 0.1 mg/ml streptomycin (Biochrom, Berlin, Germany)) till 40 % confluence. At this stage Calu-3 cells had grown in patches composed of 500-4,000 µm² with single cell covering approximatively 100 µm². The coverslips were placed in a perfusion chamber containing about 400 µl NaCl bath solution (NaCl-BS) containing 121 mM NaCl, 5.4 mM KCl, 6 mM $NaHCO_3$, 5.5 mM glucose, 0.8 mM $MgCl_2$, 2 mM $CaCl_2$, 25 mM HEPES (pH 7.4, 295 mOsmol/l) and mounted on an Eclipse Ti microscope (Nikon GmbH) equipped with an Orca flash 4.0 CCD camera (Hamamatsu Photonics Germany). Regions of interest (ROIs), corresponding mostly to single cells for N2A or Hela cells and to cell patches for Calu-3 cells, were selected. Thereafter the cells were perfused with Etd containing NaCl-BS as described above and the recording of the fluorescence images was started. Fluorescent images were taken every 15 s with an exposure time of 900 ms, 40 x or 20 x objective, dependent on the cell type (N2A, HeLa 40 x, Calu-3 20 x). For acquisition analysis and storage of the images NIS-Elements AR 4.4 software (Nikon GmbH) was used. For the superfusion of the different media onto the cells, the ISMATEC REGIO ICC peristaltic pump (Cole-Parmer GmbH, Wertheim, Germany) was used to maintain a constant 500 µl/min medium flow rate. After a recording time of about 3 minutes the cells were superfused with Etd containing NaCl-BS without Ca^{2+}. The agents CVB2-61 and CVB4-57 were tested in Ca^{2+}-free Etd containing NaCl-BS. The rate of dye uptake was estimated by considering the dye uptake within the first minute of the respective perfusion steps.

4.6. Transepithelial electrical restistance (TEER) measurement

For the TEER measurements 10^5 Calu-3 cells were seeded in transwell inserts (0.3 cm²) with a transparent porous PET membrane with pores of: 0.4 µm in diameter (BD Falcon, Corning) and cultivated in the same cell culture medium as described above for 3 days. Thereafter, they were transferred into the cellZscope+ (nanoAnalytics, Muenster, Germany) and placed in the cell culture incubator for a continuous monitoring of the TEER by impedance spectroscopy. After formation of a stable barrier of more than 1000 Ωcm² (approximately 5 days) the compounds CBX (100 µM), CVB2-61 (20 µM) or CVB4-57 (20 µM) were applied and the resistance was monitored for further 24 h.

4.7. Gold nanoparticle mediated laser perforation/dye transfer (GNOME-LP/ DT)

GNOME-LP/ DT experiments were performed as previously described [11], [40]. The cells were seeded at a density of 10^5 cells/well in 96 multiwell plates and cultivated for 72 h till confluence. Gold nanoparticles (AuNPs, diameter 200 nm, 0.5 µg/cm2) were added 3 h before an experiment started. Cells were washed with a Ca^{2+}-free NaCl-BS as described above. The laser permeabilisation was performed in presence of 0.25% Lucifer yellow (LY) dissolved in Ca^{2+}-free NaCl-BS using the laser set-up and parameters previously published [62]. In each well of a 96 multiwell plate, a line of cells was optoperforated by a 20 mW laser beam with a diameter of 60 µm and a scanning velocity of 50 mm/s. After 10 min dye diffusion time, the cells were washed with Ca^{2+}-containing bath solution and then fixed with 4% formaldehyde. In some experiments CBX (100 µM), CVB2-61 (20 µM) or CVB4-57 (20 µM) was present during optoperforation in the dye. To automatically document the GNOME LP/DT experiments, images were obtained with an Orca Flash 4.0 camera mounted onto an Eclipse Ti microscope (Nikon) with a 10 x objective using the NIS elements AR 4.21 software (Nikon). The tool Multipoint ND acquisition was used to generate three images with 2044 × 2048 pixels (1348.4 × 1351.04 µm) per well along the perforated fluorescent cell band. To analyse the diffusion distance in fluorescence plot profiles, a lab-based ImageJ plugin was used which generated a one pic of the three images included a background subtraction and Gaussian fitting, results with a R^2 value < 0.96 were not used.

4.8. Statistical analyses

 doi:10.20944/preprints202209.0120.v1

Experiments were repeated 3 – 9 times independently. All statistical analysis was performed using Microsoft Excel software (Microsoft Office 2016) and Origin software (OriginLab 7.0). One-way ANOVA were performed for all studies with $p < 0.05$ as the minimal cutoff for statistical significance. The data are given as mean with the error bars to indicate the standard deviation (SD) or standard error of the mean (SEM).

5. Conclusion

The present paper identifies Cx and specifically Cx26 hemichannels as target for the bioactive phenolic agents CVB2-61 and CVB4-57. The blocking of Cx hemichannels in epithelial cells could be a way to reduce the release of DAMPs like nucleotides by the epithelial cells during inflammatory events and may represent, at least partly, the mode of the anti-inflammatory effect of phenolic agents. The results show that CVB2-61 and CVB4-57 reversibly blocked the Cx26 hemichannels without affecting the gap junction communication or the barrier function of the epithelial cells. The results suggest a role of epithelial cells and Cx hemichannels in the discussed positive effects of phenolic agents in treatment of inflammation. In this context CVB2-61 and CVB4-57 could be a start point for further investigation for Cx hemichannel-based therapy for different pathologies that involve Cx hemichannels.

Supplementary Materials: The following supporting information can be downloaded at: www.mdpi.com/xxx/s1, Figure S1: Expression of the connexin variants in the N2A and HeLa cells. Figure S2a: Dye uptake in N2A and HeLa cells expressing only GFP and in non-transfected cells. Figure S2b: Dye uptake in HeLa cells expressing connexins. Figure S3: Representative experiments showing inhibition of the dye uptake by CVB2-61 or CVB4-57 in N2A cells expressing Cx26 and Cx46. Figure S4: Representative experiments showing dye uptake and its inhibition by CVB2-61 or CVB4-57 in Calu-3 cells.

Preprints (www.preprints.org) | NOT PEER-REVIEWED | Posted: 8 September 2022 doi:10.20944/preprints202209.0120.v1

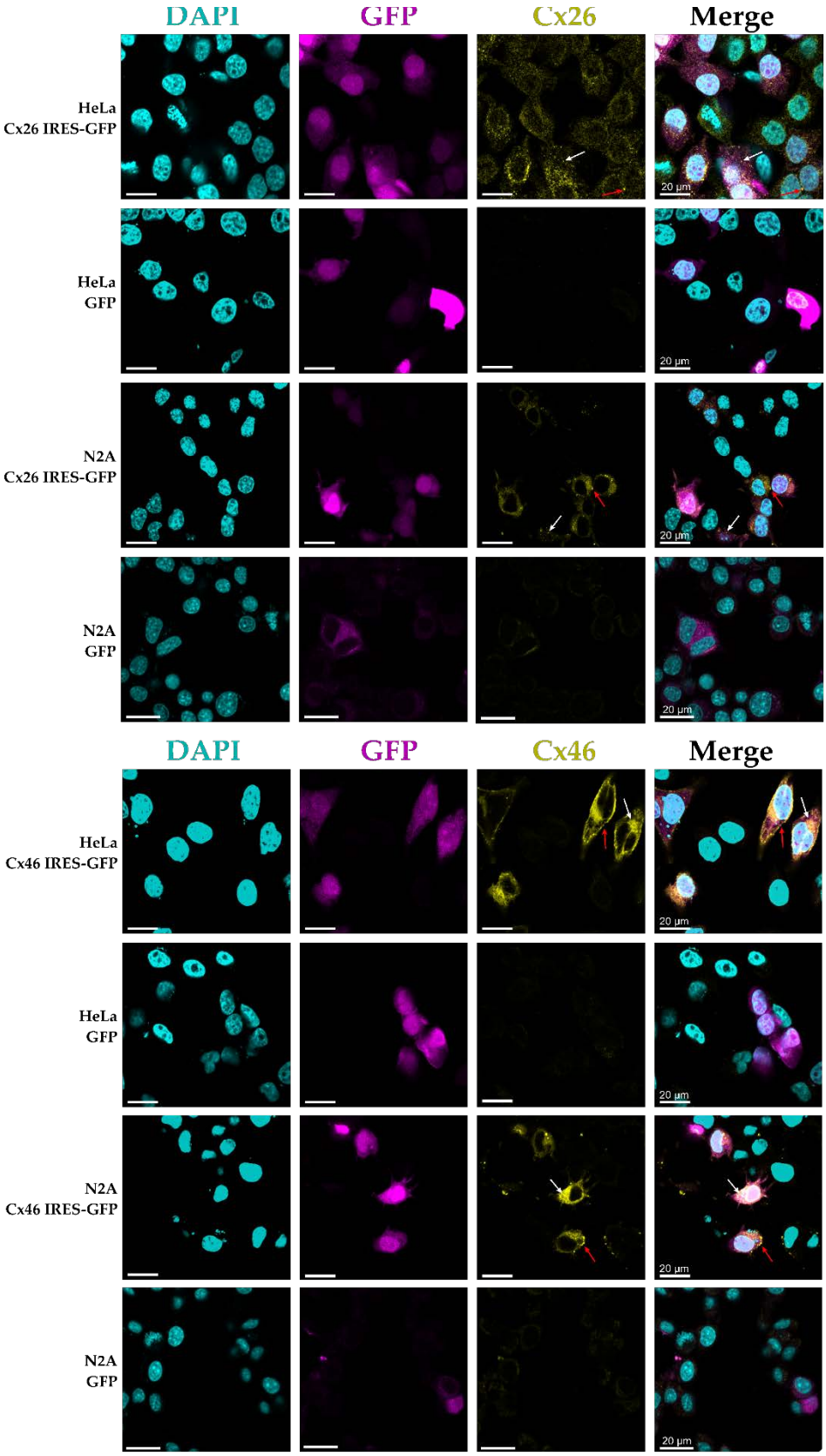

Figure S1. Expression of the connexin variants in the N2A cells and HeLa cells. Transfected cells were recognized by the expression of GFP (magenta) in the cell cytoplasm. For orientation the cell nuclei (cyan) were stained with DAPI. The Cx (yellow) were stained using respective antibodies. Cxs were mostly found at the cell border (red arrows). Cytoplasmic localization (white arrows) in structures probably vesicles, endoplasmic reticulum or Golgi apparatus was also observed.

Preprints (www.preprints.org) | NOT PEER-REVIEWED | Posted: 8 September 2022 doi:10.20944/preprints202209.0120.v1

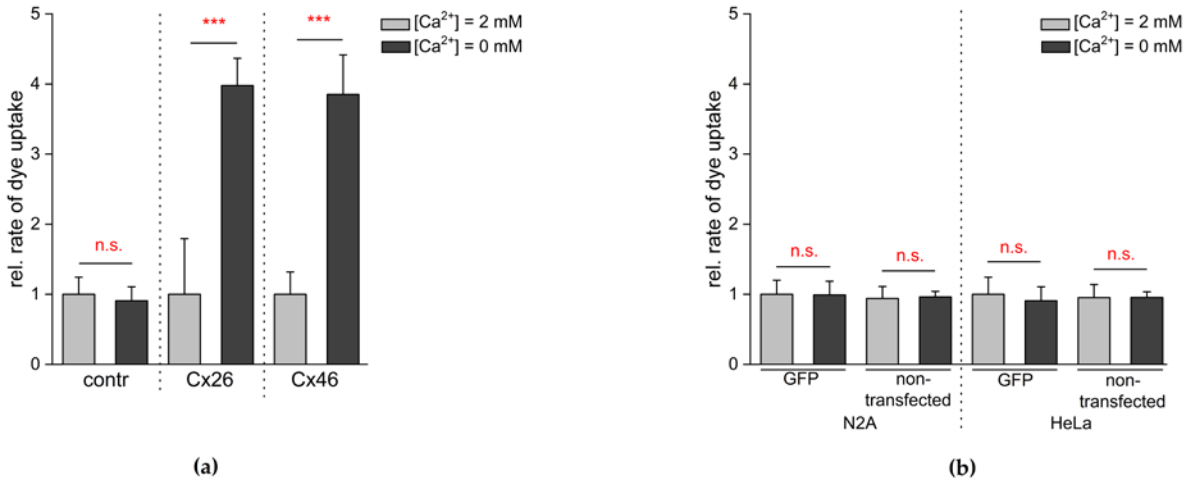

Figure S2. (**a**) Expression of GFP did not change dye uptake. Quantification of the Etd uptake in non-transfected and GFP containing vector transfected N2A and HeLa cells. Independently of the transfection, the removing of external Ca^{2+} did not markedly change the rate of dye uptake. The results are given as mean ± SEM of at least three respective and independent transfections. One-way ANOVA was applied for statistical significance to the representative control. (**b**) Dye uptake in HeLa cells expressing connexins. Quantification of the rate of Etd uptake in the HeLa cells in the presence and after removing of external Ca^{2+}. The rate of dye uptake was enhanced in HeLa cells transfected with Cx IRES-GFP variants as compared to cells only expressing GFP (contr). The results are given as average ± SEM of at least three respective experiments. One-way ANOVA was applied for statistical significance to the control (***: $p < 0.001$).

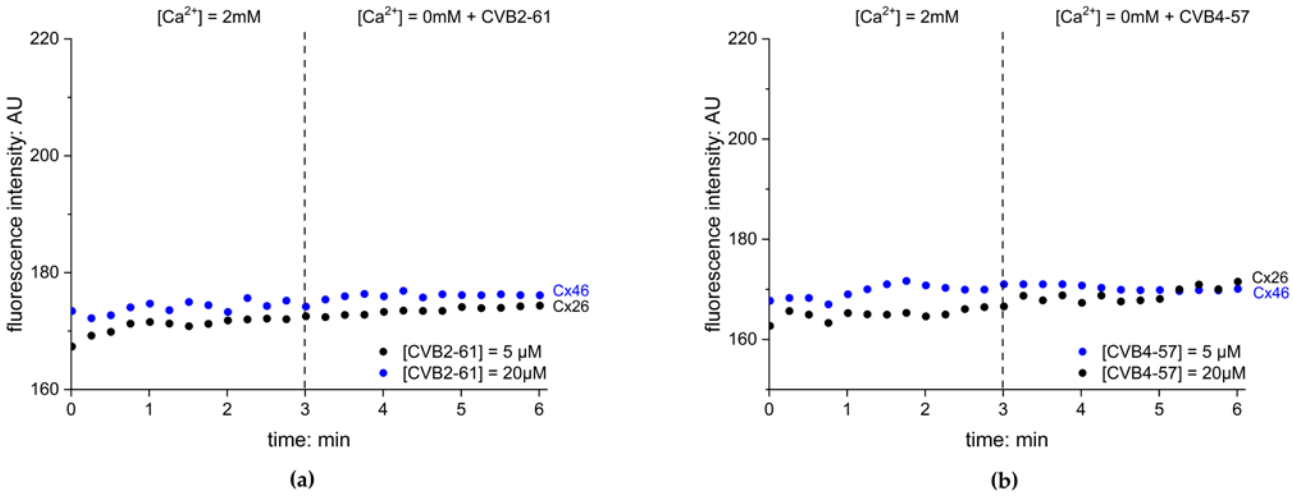

Figure S3. Inhibition of dye uptake by the agents CVB2-61 or CVB4-57. Representative experiments showing the time course of the fluorescence intensity of Etd in N2A cells transfected with hCx26IRES-GFP (Cx26) vector or Cx46IRES-GFP vector (Cx46) in presence and after removal of external Ca^{2+} in presence of CVB2-61 or CVB4-57 at the indicated concentrations.

 doi:10.20944/preprints202209.0120.v1

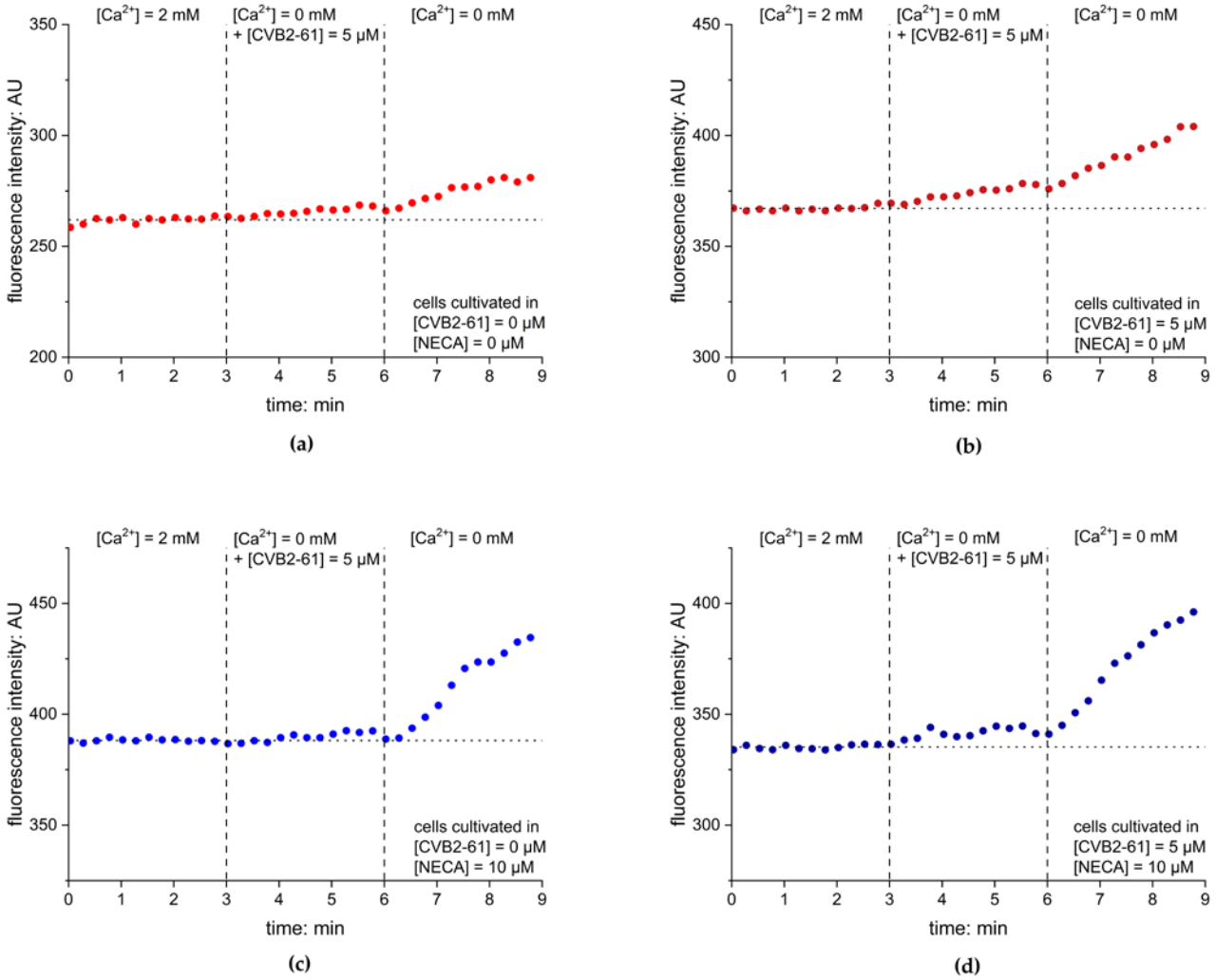

Figure S4. CVB2-61 and CVB4-57 inhibited the dye uptake in Calu-3 cells. Representative experiments showing the time course of the fluorescence intensity of Etd in Calu-3 cells treated as indicated.

Author Contributions: Participated in research design: A.N., F.B-B., C.V.-B., A.D. Conducted experiments: C.V.-B., A.D., A.S, and T.L. Performed data analysis: A.D., A.S., and T.L. Writing of the manuscript: A.N., F.B.-B., C.V.-B., A.D., P.S. The CVB2-61 and CVB4-57 for the experiments were synthetized by C.V.-B., F.B.-B. Design and generation of the vectors for the transfection experiments were performed by P.S., F.R., A.S. All authors have read and agreed to the published version of the manuscript.

Funding: This research was funded by the PhD Completion Grant programme of Hochschulbüro für ChancenVielfalt, Leibniz Universität Hannover.

Data Availability Statement: The datasets used and analysed during the current study are available from the corresponding author on request.

Acknowledgments: We thank Vicky Kawalek for the GNOME-LP/ DT macro and Frank Koepke, Helma Feierabend for technical support.

Conflicts of Interest: The authors declare no conflict of interest.

References

1. Goodenough, D.A.; Paul, D.L. Gap junctions. *Cold Spring Harb. Perspect. Biol.* **2009**, *1*, a002576, doi:10.1101/cshperspect.a002576.
2. Esseltine, J.L.; Laird, D.W. Next-Generation Connexin and Pannexin Cell Biology. *Trends Cell Biol.* **2016**, *26*, 944–955, doi:10.1016/j.tcb.2016.06.003.
3. Maeda, S.; Tsukihara, T. Structure of the gap junction channel and its implications for its biological functions. *Cell. Mol. Life Sci.* **2011**, *68*, 1115–1129, doi:10.1007/s00018-010-0551-z.
4. Sáez, J.C.; Retamal, M.A.; Basilio, D.; Bukauskas, F.F.; Bennett, M.V.L. Connexin-based gap junction hemichannels: Gating mechanisms. *Biochim. Biophys. Acta* **2005**, *1711*, 215–224, doi:10.1016/j.bbamem.2005.01.014.
5. Huang, X.; Su, Y.; Wang, N.; Li, H.; Li, Z.; Yin, G.; Chen, H.; Niu, J.; Yi, C. Astroglial Connexins in Neurodegenerative Diseases. *Front. Mol. Neurosci.* **2021**, *14*, 657514, doi:10.3389/fnmol.2021.657514.
6. Orellana, J.A.; Bernhardi, R. von; Giaume, C.; Sáez, J.C. Glial hemichannels and their involvement in aging and neurodegenerative diseases. *Rev. Neurosci.* **2012**, *23*, 163–177, doi:10.1515/revneuro-2011-0065.
7. Ramadan, R.; Vromans, E.; Anang, D.C.; Goetschalckx, I.; Hoorelbeke, D.; Decrock, E.; Baatout, S.; Leybaert, L.; Aerts, A. Connexin43 Hemichannel Targeting With TAT-Gap19 Alleviates Radiation-Induced Endothelial Cell Damage. *Front. Pharmacol.* **2020**, *11*, 212, doi:10.3389/fphar.2020.00212.
8. Pfenniger, A.; Chanson, M.; Kwak, B.R. Connexins in atherosclerosis. *Biochim. Biophys. Acta* **2013**, *1828*, 157–166, doi:10.1016/j.bbamem.2012.05.011.
9. Willebrords, J.; Crespo Yanguas, S.; Maes, M.; Decrock, E.; Wang, N.; Leybaert, L.; Kwak, B.R.; Green, C.R.; Cogliati, B.; Vinken, M. Connexins and their channels in inflammation. *Crit. Rev. Biochem. Mol. Biol.* **2016**, *51*, 413–439, doi:10.1080/10409238.2016.1204980.
10. Schalper, K.A.; Carvajal-Hausdorf, D.; Oyarzo, M.P. Possible role of hemichannels in cancer. *Front. Physiol.* **2014**, *5*, 237, doi:10.3389/fphys.2014.00237.
11. Dierks, A.; Bader, A.; Lehrich, T.; Ngezahayo, A. Stimulation of the A2B Adenosine Receptor Subtype Enhances Connexin26 Hemichannel Activity in Small Airway Epithelial Cells. *Cell. Physiol. Biochem.* **2019**, *53*, 606–622, doi:10.33594/000000160.
12. García-Vega, L.; O'Shaughnessy, E.M.; Jan, A.; Bartholomew, C.; Martin, P.E. Connexin 26 and 43 play a role in regulating proinflammatory events in the epidermis. *J. Cell. Physiol.* **2019, doi:**10.1002/jcp.28206.
13. Mugisho, O.O.; Green, C.R.; Kho, D.T.; Zhang, J.; Graham, E.S.; Acosta, M.L.; Rupenthal, I.D. The inflammasome pathway is amplified and perpetuated in an autocrine manner through connexin43 hemichannel mediated ATP release. *Biochim. Biophys. Acta Gen. Subj.* **2018**, *1862*, 385–393, doi:10.1016/j.bbagen.2017.11.015+.
14. Liu, J.; Riquelme, M.A.; Li, Z.; Li, Y.; Tong, Y.; Quan, Y.; Pei, C.; Gu, S.; Jiang, J.X. Mechanosensitive collaboration between integrins and connexins allows nutrient and antioxidant transport into the lens. *J. Cell Biol.* **2020**, *219, doi:*10.1083/jcb.202002154.
15. Plotkin, L.I. Connexin 43 hemichannels and intracellular signaling in bone cells. *Front. Physiol.* **2014**, *5*, 131, doi:10.3389/fphys.2014.00131.
16. Vinken, M. Connexin hemichannels: Novel mediators of toxicity. *Arch. Toxicol.* **2015**, *89*, 143–145, doi:10.1007/s00204-014-1422-4.
17. Wang, N.; Bock, M. de; Decrock, E.; Bol, M.; Gadicherla, A.; Vinken, M.; Rogiers, V.; Bukauskas, F.F.; Bultynck, G.; Leybaert, L. Paracrine signaling through plasma membrane hemichannels. *Biochim. Biophys. Acta* **2013**, *1828*, 35–50, doi:10.1016/j.bbamem.2012.07.002.

18. Buratto, D.; Donati, V.; Zonta, F.; Mammano, F. Harnessing the therapeutic potential of antibodies targeting connexin hemichannels. *Biochim. Biophys. Acta Mol. Basis Dis.* **2021**, *1867*, 166047, doi:10.1016/j.bbadis.2020.166047.
19. Tang, D.; Kang, R.; Coyne, C.B.; Zeh, H.J.; Lotze, M.T. PAMPs and DAMPs: Signal 0s that spur autophagy and immunity. *Immunol. Rev.* **2012**, *249*, 158–175, doi:10.1111/j.1600-065X.2012.01146.x.
20. Burgoyne, R.A.; Fisher, A.J.; Borthwick, L.A. The Role of Epithelial Damage in the Pulmonary Immune Response. *Cells* **2021**, *10, doi:*10.3390/cells10102763.
21. Johnston, S.L.; Goldblatt, D.L.; Evans, S.E.; Tuvim, M.J.; Dickey, B.F. Airway Epithelial Innate Immunity. *Front. Physiol.* **2021**, *12*, 749077, doi:10.3389/fphys.2021.749077.
22. Vuyst, E. de; Decrock, E.; Bock, M. de; Yamasaki, H.; Naus, C.C.; Evans, W.H.; Leybaert, L. Connexin hemichannels and gap junction channels are differentially influenced by lipopolysaccharide and basic fibroblast growth factor. *Mol. Biol. Cell* **2007**, *18*, 34–46, doi:10.1091/mbc.e06-03-0182.
23. Li, C.; Miao, X.; Li, F.; Adhikari, B.K.; Liu, Y.; Sun, J.; Zhang, R.; Cai, L.; Liu, Q.; Wang, Y. Curcuminoids: Implication for inflammation and oxidative stress in cardiovascular diseases. *Phytother. Res.* **2019**, *33*, 1302–1317, doi:10.1002/ptr.6324.
24. He, Y.; Yue, Y.; Zheng, X.; Zhang, K.; Chen, S.; Du, Z. Curcumin, inflammation, and chronic diseases: How are they linked? *Molecules* **2015**, *20*, 9183–9213, doi:10.3390/molecules20059183.
25. Salehi, B.; Stojanović-Radić, Z.; Matejić, J.; Sharifi-Rad, M.; Anil Kumar, N.V.; Martins, N.; Sharifi-Rad, J. The therapeutic potential of curcumin: A review of clinical trials. *Eur. J. Med. Chem.* **2019**, *163*, 527–545, doi:10.1016/j.ejmech.2018.12.016.
26. Estornut, C.; Milara, J.; Bayarri, M.A.; Belhadj, N.; Cortijo, J. Targeting Oxidative Stress as a Therapeutic Approach for Idiopathic Pulmonary Fibrosis. *Front. Pharmacol.* **2021**, *12*, 794997, doi:10.3389/fphar.2021.794997.
27. Liu, Z.; Ying, Y. The Inhibitory Effect of Curcumin on Virus-Induced Cytokine Storm and Its Potential Use in the Associated Severe Pneumonia. *Front. Cell Dev. Biol.* **2020**, *8*, 479, doi:10.3389/fcell.2020.00479.
28. Yahfoufi, N.; Alsadi, N.; Jambi, M.; Matar, C. The Immunomodulatory and Anti-Inflammatory Role of Polyphenols. *Nutrients* **2018**, *10, doi:*10.3390/nu10111618.
29. Vanucci-Bacqué, C.; Camare, C.; Carayon, C.; Bernis, C.; Baltas, M.; Nègre-Salvayre, A.; Bedos-Belval, F. Synthesis and evaluation of antioxidant phenolic diaryl hydrazones as potent antiangiogenic agents in atherosclerosis. *Bioorg. Med. Chem.* **2016**, *24*, 3571–3578, doi:10.1016/j.bmc.2016.05.067.
30. Beyer, E.C.; Berthoud, V.M. Connexin hemichannels in the lens. *Front. Physiol.* **2014**, *5*, 20, doi:10.3389/fphys.2014.00020.
31. Sellitto, C.; Li, L.; White, T.W. Connexin hemichannel inhibition ameliorates epidermal pathology in a mouse model of keratitis ichthyosis deafness syndrome. *Sci. Rep.* **2021**, *11*, 24118, doi:10.1038/s41598-021-03627-8.
32. Maeda, S.; Nakagawa, S.; Suga, M.; Yamashita, E.; Oshima, A.; Fujiyoshi, Y.; Tsukihara, T. Structure of the connexin 26 gap junction channel at 3.5 A resolution. *Nature* **2009**, *458*, 597–602, doi:10.1038/nature07869.
33. Schadzek, P.; Schlingmann, B.; Schaarschmidt, F.; Lindner, J.; Koval, M.; Heisterkamp, A.; Ngezahayo, A.; Preller, M. Data of the molecular dynamics simulations of mutations in the human connexin46 docking interface. *Data Brief* **2016**, *7*, 93–99, doi:10.1016/j.dib.2016.01.067.
34. Schadzek, P.; Hermes, D.; Stahl, Y.; Dilger, N.; Ngezahayo, A. Concatenation of Human Connexin26 (hCx26) and Human Connexin46 (hCx46) for the Analysis of Heteromeric Gap Junction Hemichannels and Heterotypic Gap Junction Channels. *Int. J. Mol. Sci.* **2018**, *19, doi:*10.3390/ijms19092742.

35. Schalper, K.A.; Palacios-Prado, N.; Retamal, M.A.; Shoji, K.F.; Martínez, A.D.; Sáez, J.C. Connexin hemichannel composition determines the FGF-1-induced membrane permeability and free Ca2+i responses. *Mol. Biol. Cell* **2008**, *19*, 3501–3513, doi:10.1091/mbc.e07-12-1240.
36. Johnson, R.G.; Le, H.C.; Evenson, K.; Loberg, S.W.; Myslajek, T.M.; Prabhu, A.; Manley, A.-M.; O'Shea, C.; Grunenwald, H.; Haddican, M.; et al. Connexin Hemichannels: Methods for Dye Uptake and Leakage. *J. Membr. Biol.* **2016**, *249*, 713–741, doi:10.1007/s00232-016-9925-y.
37. Zhu, Y.; Chidekel, A.; Shaffer, T.H. Cultured human airway epithelial cells (calu-3): A model of human respiratory function, structure, and inflammatory responses. *Crit. Care Res. Pract.* **2010**, *2010, doi:*10.1155/2010/394578.
38. Kreft, M.E.; Jerman, U.D.; Lasič, E.; Hevir-Kene, N.; Rižner, T.L.; Peternel, L.; Kristan, K. The characterization of the human cell line Calu-3 under different culture conditions and its use as an optimized in vitro model to investigate bronchial epithelial function. *Eur. J. Pharm. Sci.* **2015**, *69*, 1–9, doi:10.1016/j.ejps.2014.12.017.
39. Foster, K.A.; Avery, M.L.; Yazdanian, M.; Audus, K.L. Characterization of the Calu-3 cell line as a tool to screen pulmonary drug delivery. *International Journal of Pharmaceutics* **2000**, *208*, 1–11, doi:10.1016/S0378-5173(00)00452-X.
40. Begandt, D.; Bader, A.; Antonopoulos, G.C.; Schomaker, M.; Kalies, S.; Meyer, H.; Ripken, T.; Ngezahayo, A. Gold nanoparticle-mediated (GNOME) laser perforation: A new method for a high-throughput analysis of gap junction intercellular coupling. *J. Bioenerg. Biomembr.* **2015**, *47*, 441–449, doi:10.1007/s10863-015-9623-y.
41. Buckley, C.; Zhang, X.; Wilson, C.; McCarron, J.G. Carbenoxolone and 18β-glycyrrhetinic acid inhibit inositol 1,4,5-trisphosphate-mediated endothelial cell calcium signalling and depolarise mitochondria. *Br. J. Pharmacol.* **2021**, *178*, 896–912, doi:10.1111/bph.15329.
42. Malekinejad, M.; Pashaee, M.R.; Malekinejad, H. 18β-Glycyrrhetinic acid altered the intestinal permeability in the human Caco-2 monolayer cell model. *Eur. J. Nutr.* **2022, doi:**10.1007/s00394-022-02900-4.
43. Arzola-Martínez, L.; Benavente, R.; Vega, G.; Ríos, M.; Fonseca, W.; Rasky, A.J.; Morris, S.; Lukacs, N.W.; Villalón, M.J. Blocking ATP-releasing channels prevents high extracellular ATP levels and airway hyperreactivity in an asthmatic mouse model. *Am. J. Physiol. Lung Cell. Mol. Physiol.* **2021**, *321*, L466-L476, doi:10.1152/ajplung.00450.2020.
44. Zhang, J.; O'Carroll, S.J.; Henare, K.; Ching, L.-M.; Ormonde, S.; Nicholson, L.F.B.; Danesh-Meyer, H.V.; Green, C.R. Connexin hemichannel induced vascular leak suggests a new paradigm for cancer therapy. *FEBS Lett.* **2014**, *588*, 1365–1371, doi:10.1016/j.febslet.2014.02.003.
45. Bodendiek, S.B.; Raman, G. Connexin modulators and their potential targets under the magnifying glass. *Curr. Med. Chem.* **2010**, *17*, 4191–4230, doi:10.2174/092986710793348563.
46. Willebrords, J.; Maes, M.; Crespo Yanguas, S.; Vinken, M. Inhibitors of connexin and pannexin channels as potential therapeutics. *Pharmacol. Ther.* **2017**, *180*, 144–160, doi:10.1016/j.pharmthera.2017.07.001.
47. Yi, C.; Ezan, P.; Fernández, P.; Schmitt, J.; Sáez, J.C.; Giaume, C.; Koulakoff, A. Inhibition of glial hemichannels by boldine treatment reduces neuronal suffering in a murine model of Alzheimer's disease. *Glia* **2017**, *65*, 1607–1625, doi:10.1002/glia.23182.
48. Abudara, V.; Bechberger, J.; Freitas-Andrade, M.; Bock, M. de; Wang, N.; Bultynck, G.; Naus, C.C.; Leybaert, L.; Giaume, C. The connexin43 mimetic peptide Gap19 inhibits hemichannels without altering gap junctional communication in astrocytes. *Front. Cell. Neurosci.* **2014**, *8*, 306, doi:10.3389/fncel.2014.00306.
49. Fiori, M.C.; Krishnan, S.; Kjellgren, A.; Cuello, L.G.; Altenberg, G.A. Inhibition by Commercial Aminoglycosides of Human Connexin Hemichannels Expressed in Bacteria. *Molecules* **2017**, *22, doi:*10.3390/molecules22122063.

50. Natha, C.M.; Vemulapalli, V.; Fiori, M.C.; Chang, C.-W.T.; Altenberg, G.A. Connexin hemichannel inhibitors with a focus on aminoglycosides. *Biochim. Biophys. Acta Mol. Basis Dis.* **2021**, *1867*, 166115, doi:10.1016/j.bbadis.2021.166115.
51. Xu, L.; Carrer, A.; Zonta, F.; Qu, Z.; Ma, P.; Li, S.; Ceriani, F.; Buratto, D.; Crispino, G.; Zorzi, V.; et al. Design and Characterization of a Human Monoclonal Antibody that Modulates Mutant Connexin 26 Hemichannels Implicated in Deafness and Skin Disorders. *Front. Mol. Neurosci.* **2017**, *10*, 298, doi:10.3389/fnmol.2017.00298.
52. AlFindee, M.N.; Subedi, Y.P.; Fiori, M.C.; Krishnan, S.; Kjellgren, A.; Altenberg, G.A.; Chang, C.-W.T. Inhibition of Connexin Hemichannels by New Amphiphilic Aminoglycosides without Antibiotic Activity. *ACS Med. Chem. Lett.* **2018**, *9*, 697–701, doi:10.1021/acsmedchemlett.8b00158.
53. Costantino, V.; Fattorusso, E.; Mangoni, A.; Perinu, C.; Teta, R.; Panza, E.; Ianaro, A. Tedarenes A and B: Structural and stereochemical analysis of two new strained cyclic diarylheptanoids from the marine sponge Tedania ignis. *J. Org. Chem.* **2012**, *77*, 6377–6383, doi:10.1021/jo300295j.
54. Maurent, K.; Vanucci-Bacqué, C.; Baltas, M.; Nègre-Salvayre, A.; Augé, N.; Bedos-Belval, F. Synthesis and biological evaluation of diarylheptanoids as potential antioxidant and anti-inflammatory agents. *Eur. J. Med. Chem.* **2018**, *144*, 289–299, doi:10.1016/j.ejmech.2017.12.033.
55. Kumar, N.; Goel, N. Phenolic acids: Natural versatile molecules with promising therapeutic applications. *Biotechnol. Rep. (Amst)* **2019**, *24*, e00370, doi:10.1016/j.btre.2019.e00370.
56. Enders, O.; Ngezahayo, A.; Wiechmann, M.; Leisten, F.; Kolb, H.-A. Structural calorimetry of main transition of supported DMPC bilayers by temperature-controlled AFM. *Biophys. J.* **2004**, *87*, 2522–2531, doi:10.1529/biophysj.104.040105.
57. Takens-Kwak, B.R.; Jongsma, H.J.; Rook, M.B.; van Ginneken, A.C. Mechanism of heptanol-induced uncoupling of cardiac gap junctions: A perforated patch-clamp study. *Am. J. Physiol.* **1992**, *262*, C1531-8, doi:10.1152/ajpcell.1992.262.6.C1531.
58. Bastiaanse, E.M.; Jongsma, H.J.; van der Laarse, A.; Takens-Kwak, B.R. Heptanol-induced decrease in cardiac gap junctional conductance is mediated by a decrease in the fluidity of membranous cholesterol-rich domains. *J. Membr. Biol.* **1993**, *136*, 135–145, doi:10.1007/BF02505758.
59. Evans, W.H.; Boitano, S. Connexin mimetic peptides: Specific inhibitors of gap-junctional intercellular communication. *Biochem. Soc. Trans.* **2001**, *29*, 606–612, doi:10.1042/bst0290606.
60. Schadzek, P.; Stahl, Y.; Preller, M.; Ngezahayo, A. Analysis of the dominant mutation N188T of human connexin46 (hCx46) using concatenation and molecular dynamics simulation. *FEBS Open Bio* **2019**, *9*, 840–850, doi:10.1002/2211-5463.12624.
61. Gubbels, S.P.; Woessner, D.W.; Mitchell, J.C.; Ricci, A.J.; Brigande, J.V. Functional auditory hair cells produced in the mammalian cochlea by in utero gene transfer. *Nature* **2008**, *455*, 537–541, doi:10.1038/nature07265.
62. Heinemann, D.; Schomaker, M.; Kalies, S.; Schieck, M.; Carlson, R.; Murua Escobar, H.; Ripken, T.; Meyer, H.; Heisterkamp, A. Gold nanoparticle mediated laser transfection for efficient siRNA mediated gene knock down. *PLoS One* **2013**, *8*, e58604, doi:10.1371/journal.pone.0058604.